IDA

INSTITUTE FOR DEFENSE ANALYSES

Ultra-Wide SAR System Analysis

James M. Ralston

September 1998

IDA Document D-2199

Log: H 98-002557

PREFACE

This work was undertaken for the Defense Advanced Research Projects Agency under a task entitled "Counter Camouflage Concealment and Deception (CCC&D) Systems Studies" as part of the program to develop ultra-wideband radar technology for detecting hostile targets that may be covered, concealed, or camouflaged. This document was originally presented at the EUSAR 98 SAR Conference in Friedrichshafen, Germany, on 25 May 1998, and is published in the conference proceedings.

Ultra-Wide SAR System Analysis*

James M. Ralston, The Institute for Defense Analyses, Alexandria, Virginia 22311

Abstract*

This paper develops a methodology for analyzing the performance of ultra-wide SAR systems that relaxes the approximations commonly carried over from narrow-band/beam SAR analysis. The analysis is applied to system sensitivity and resolution calculations

1. Introduction

In recent years the achievements of airborne SAR using microwave frequencies have been complemented by the development of high-resolution SAR at much lower frequencies in the VHF and UHF bands.[1] The combination of wide bandwidth and low carrier frequency leads to the characterization of such SARs as *ultra-wideband* (UWB). Unlike SAR at higher frequency, which employ collection beamwidths of only a few degrees in strip-map mode, UWB SAR routinely uses collection angles of more than 30 degrees, so it is correct to characterize these systems as *ultra-widebeam* as well. This paper will present a consistent methodology for analyzing the system sensitivity and resolution of *ultra-wide* (band and beam) SARs.

The conventional approach to the system analysis of strip-map synthetic aperture radar has routinely made two key approximations: 1)Low fractional bandwidth. This permits approximating key system variables, such as transmit power spectrum, antenna pattern, SAR collection angle, system noise, etc, which are inherently frequency dependent, by single mean values. 2)Narrow antenna beamwidth. This permits neglecting the variation in $1/R^4$ over the synthetic aperture, as well as any obliquity factors or other spatial structure in the antenna pattern.

Despite these limitations, conventional narrow-band/narrow-beam SAR equations have been widely applied to ultra-wideband/widebeam SAR in order to estimate system power, sensitivity, and collection aperture requirements. In this analysis we relax the narrow band/narrow beam approximations to develop a system analysis methodology applicable to the ultra-wideband/widebeam (UWB) case. We consider explicitly: 1)The frequency variation of each of the radar system characteristics that govern the returned signal. 2)The time variation of received radar signal power from a point pixel as the antenna moves through the synthetic aperture. This variation is due to both antenna pattern fall off and variation in $1/R^4$ over the aperture. For this reason it is necessary to employ a specific model of the antenna spatial pattern. 3)The frequency variation of system noise temperature. Unlike conventional microwave SAR for which the system noise is dominated by internal receiver noise and a generally well-behaved external noise temperature near 300 K, UWB SAR in the UHF and particularly the VHF bands must contend with external noise sources whose effective temperature can exceed 100,000 K. In this analysis we include the effects of external noise sources which are considered in detail in a companion paper.

2. System Relative Response Function

The process of SAR data collection is shown in **figure 1**.

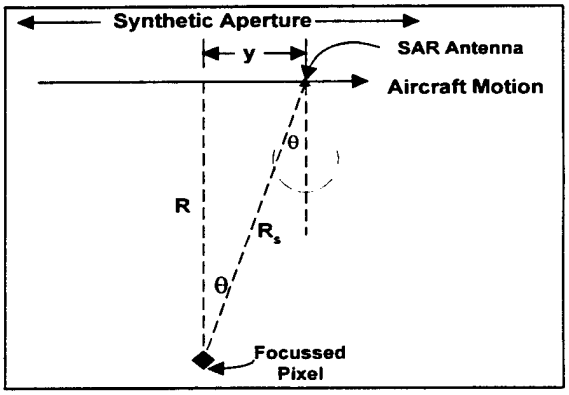

Figure 1

In the following we consider a horizontally polarized linear antenna as an example, but the patterns of other antennas can be readily substituted. At a point, y, in the synthetic aperture, the signal power received from the target, relative to the signal at the center of the aperture (y=0) is:

$$g(y,f,L_a,R) = \left[f_p(\pi L_a \frac{f}{c}\sin(\theta)) \cdot \cos(\theta) \right]^4 \times (R/R_s)^4 \qquad Eq.1$$
$$= f_p^4(\ldots)\cdot\cos(\theta)^8$$

This is the *relative response function* where the normalized antenna pattern factor, f_p can be modeled by the expression for a cosine-weighted line source:

$$f_p(u) = \frac{\cos(u)}{1-(\frac{2u}{\pi})^2}. \qquad Eq.2$$

* This work was supported by the Defense Advance Research Project Agency.

The relative response function is the target's power illumination history. For a SAR antenna with a real aperture of 1.5 m, having a minimum range of 10 km from the imaged point, this illumination history is illustrated in **figure 2** at two frequencies. We plot relative power vs position in the synthetic aperture normalized to the range, R. This illustrates some features of the response function: 1)For a the antenna pattern model used in this example, the effective length of the synthetic aperture is strongly frequency dependent and much less at the higher frequency. 2)The combination of the antenna's obliquity factor and the $1/R^4$ variation imposes an

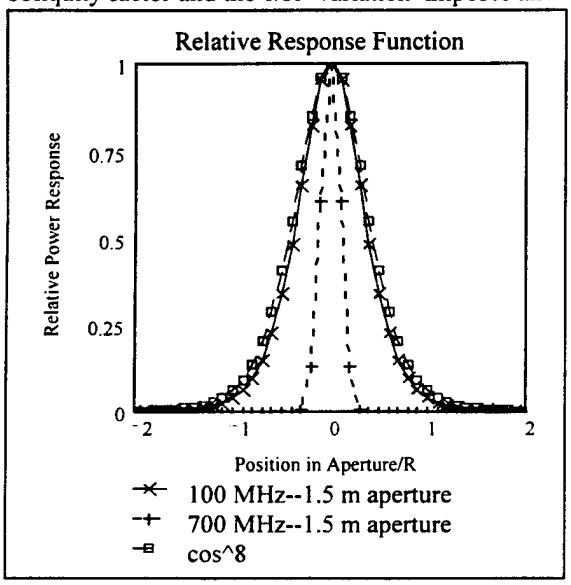

Figure 2

effective factor of $\cos^8$ on the antenna beamwidth. This sets an upper beamwidth limit of ~50 deg. (The $1/R^4$ factor alone sets an upper beamwidth limit of ~65 deg.) 3) This beamwidth limit is most significant when L/λ is small. That is, in the case of UWB SAR at VHF/UHF frequencies.

3. Effective Aperture and Scene Angle

This relative response function can be used to define several related measures relative to SAR system performance. If L_p is the processed synthetic aperture over which data is collected for imaging, then the effective synthetic aperture, l_e is defined to be:

$$l_e = \int_{-L_p/2}^{L_p/2} g(y)dy \qquad Eq.3$$

The effective synthetic aperture is always less than the processed aperture. The asymptotic effective aperture, l_∞ is defined in the limit:

$$l_\infty = \lim(L_p \to \infty) \int_{-L_p/2}^{L_p/2} g(y)dy \qquad Eq.4$$

So defined, l_∞ is a parameter of the antenna and collection geometry. It is convenient to eliminate the formal range dependence by defining an effective scene tangent, a_e and effective scene angle, θ_e:

$$a_e = l_\infty / R$$
$$\theta_e = 2 \cdot \tan^{-1}(a_e / 2) \qquad Eq.5$$

These measures are frequency-dependent through the antenna pattern. The effective scene tangent is plotted in **figure 3** for the example antenna and for a hypothetical continuously tuned half-wave dipole, which maintains a constant pattern with frequency.

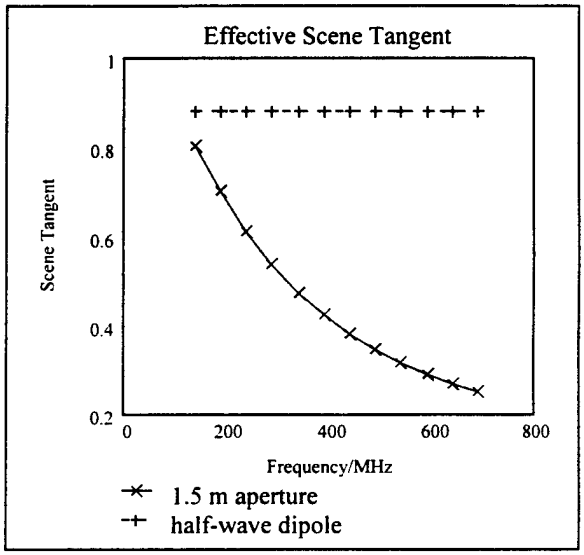

Figure 3

The effective scene angle is plotted in **figure 4** for the same two antennas along with θ_3, the nominal 3-dB beamwidth, which is often used as a measure of cross-range resolution.

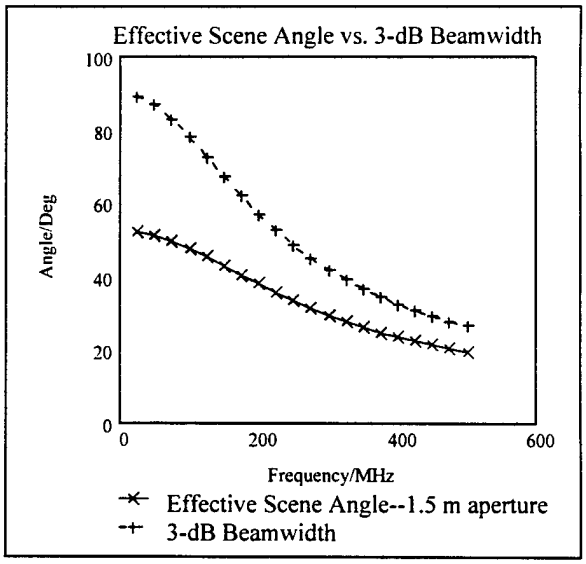

Figure 4

As can be seen, the effective scene angle, which is a measure of the angle that would account for the entire received signal energy, and is generally smaller than the angle over which energy is collected, is a much better indicator of the useful angular coverage of the system than the 3-dB antenna beamwidth.

4. Ultrawide System Losses

In ultrawide SAR the effective synthetic aperture is $R \cdot a_e$. The corresponding quantity for conventional SAR is $R \cdot \theta_3$, where θ_3 is often taken to be l/L. The ratio of apertures represents an effective ultrawide loss, L_{uw}, which accounts for $1/R^4$ variation over the synthetic aperture as well as beamshape losses that were not considered in the conventional approximation. It is plotted in **figure 5** for several cases. Inclusion of this loss component can be used to correct sensitivity estimates that employ the conventional narrowband/beam radar range equation.

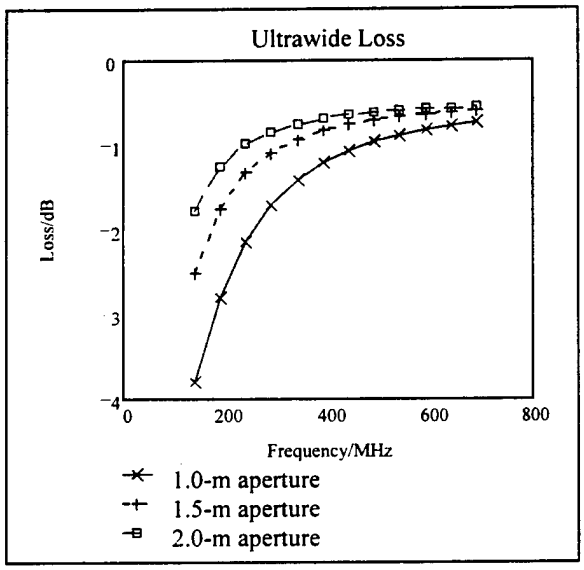

Figure 5

The losses increase at low frequency, particularly for the smaller antennas, due to the large $1/R^4$ variation over the wide synthetic aperture.

Achieving the full "effective aperture" requires collecting SAR data over an impractical infinite collection aperture. Practical processed apertures are necessarily finite, entailing some *truncation loss*. In **figure 6** we plot the calculated truncation loss (ratio of achieved effective aperture to asymptotic effective aperture) associated with a finite processed aperture expressed in units of the asymptotic effective aperture. The two cases shown correspond to antenna apertures of 1.5 and 4 metres and show that the losses expressed in this form are not strongly dependent on antenna pattern. Integrating a processed aperture equal only to the asymptotic

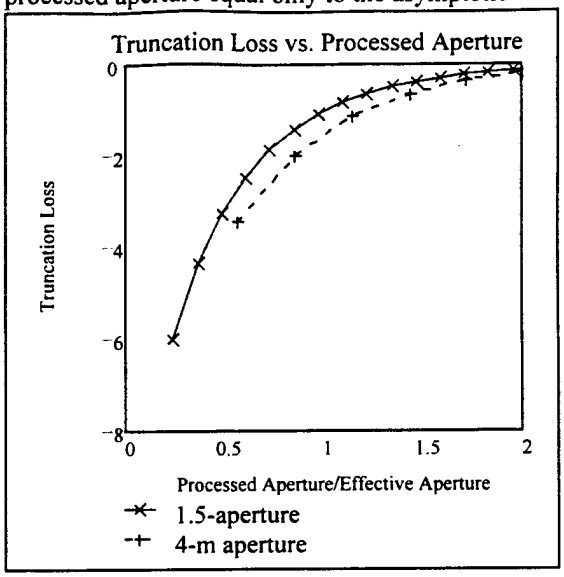

Figure 6

effective aperture leads to truncation losses of ~1-1.5 dB, while integrating two effective apertures reduces truncation losses to ~0.2 dB.

5. System Transfer Function and Impulse Response

In order to compute the system response it is necessary to invoke a more specific antenna model. We assume here that the azimuthal pattern is given by eq. 1 and that the peak gain is given by:

$$G_0(f) = \frac{16 \cdot \eta}{\theta_{3e} \cdot \theta_{3a}(f, L_a)} \qquad Eq.6$$

where the efficiency, η, is 0.5, the elevation beamwidth, θ_{3e}, is 1.1 rad and the azimuth beamwidth is obtained from eq. 1. Using eqs. 1,2 and 6, the energy density at the point (kx,ky) in wavenumber space can be shown to be : *Eq.7*

$$E_d(k_x, k_y) = (\frac{2\pi}{c})^2 G_0^2(f) f_p^4 (\frac{L_a k_y}{2}) \frac{k_x^7}{(k_x^2 + k_y^2)^5}$$

The voltage pixel response function or system transfer function is proportional to the square root of this expression and is plotted in **figure 7**. The system impulse response is given by the two dimensional Fourier transform of the transfer function, and is plotted in **figure 8**. No apodization is used in this calculation. the natural fall off of system response in the y direction due to antenna pattern and $1/R^4$ variation acts to suppress cross-range sidelobes. The assumed abrupt truncation of the spectral support at the band edges, on the other hand, leads to significant sidelobes in the range direction. The effective area of the impulse response function defines the system resolution and is given

by the two-dimensional integral of its squared value. For this example, the system resolution is 0.15 m^2.

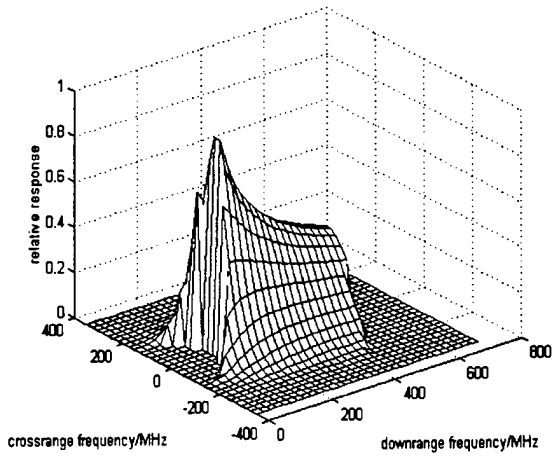

Figure 7

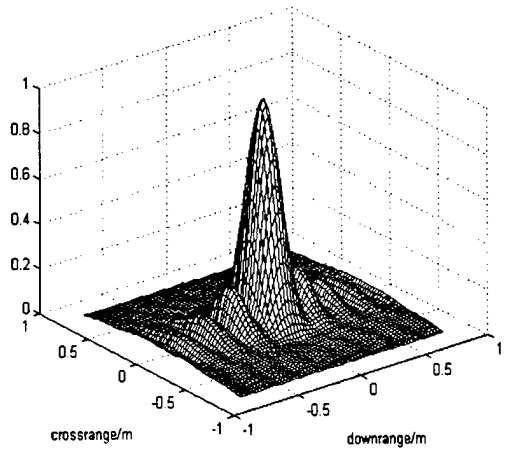

Figure 8

6. System Sensitivity

The energy collected per coherent dwell is the integral of received spectral power density over frequency and time in the aperture. With the aid of eqs. 3,4 and 5 this becomes: *Eq.8*

$$E = \frac{P_{av} c^2 \sigma}{(f_2 - f_1)(4\pi)^3 R^3 L_{RF} v} \int_{f_1}^{f_2} \frac{G_0^2(f)}{f^2} a_e(f) df$$

Here Pav/(f2-f1) is the transmitted power density, LRF is the system RF loss and v is the platform speed. For the 100-700 MHz band the effective system noise temperature is estimated in a companion paper [2] to be ~460 K. Using the system resolution obtained above we can compute the noise -equivalent clutter reflectivity ($NE\sigma_0$) for the case of Pav=60 W, L_{RF}=1.6 (2 dB) and v=175 m/sec. This is shown in fig. 9 plotted vs. range. Note that this sensitivity reflects only natural and inadvertent sources of manmade noise. Practical systems will be very much impacted by additional interference from broadcast sources.

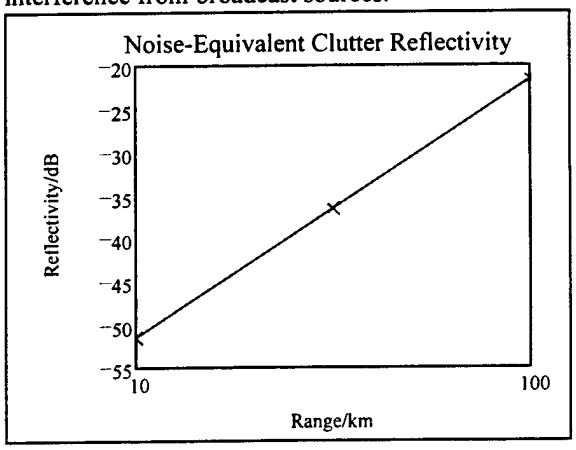

Figure 9

7. Conclusions

The many unique advantages of ultrawide SAR at VHF and UHF frequencies come with additional challenges for system designers. In particular system performance is sensitive to antenna characteristics over much wider ranges of angle and frequency than are customarily employed in microwave SARs. This paper has reported methods for systematically accounting for detailed antenna characteristics in estimating the performance characteristics of SARs.

References

[1] Ulander, Lars M.H. and Hans Helsten. A New Formula for SAR Spatial Resolution. AEU Int. J. Electon. Commun., 50, pp. 117-121 (1996).

[2] Ralston, James M., James F. Heagy and Roger Sullivan. Environmental Noise Effects on VHF/ UHF UWB SAR. Proceedings of Eusar 98. This volume (1998)

REPORT DOCUMENTATION PAGE

Form Approved
OMB No. 0704-0188

1. AGENCY USE ONLY *(Leave blank)*	2. REPORT DATE	3. REPORT TYPE AND DATES COVERED
	September 1998	Final—November 1996–June 1997

4. TITLE AND SUBTITLE
Ultra-Wide SAR System Analysis

5. FUNDING NUMBERS
DASW01 94 C 0054
Task Assignment A-155

6. AUTHOR(S)
James M. Ralston

7. PERFORMING ORGANIZATION NAME(S) AND ADDRESS(ES)
Institute for Defense Analyses
1801 N. Beauregard St.
Alexandria, VA 22311-1772

8. PERFORMING ORGANIZATION REPORT NUMBER
IDA Document D-2199

9. SPONSORING/MONITORING AGENCY NAME(S) AND ADDRESS(ES)
Defense Advanced Research Projects Agency
Information Systems Office
3701 N. Fairfax Drive
Arlington, VA 22210

10. SPONSORING/MONITORING AGENCY REPORT NUMBER

11. SUPPLEMENTARY NOTES

12a. DISTRIBUTION/AVAILABILITY STATEMENT
Approved for public release; distribution unlimited.

12b. DISTRIBUTION CODE

13. ABSTRACT ***(Maximum 180 words)***

This paper develops a methodology for analyzing the performance of ultra-wide SAR systems that relaxes the approximations commonly carried over from narrow-band/beam SAR analysis. The analysis is applied to system sensitivity and resolution calculations.

14. SUBJECT TERMS
Ultra-Wideband Radar, SAR, System Analysis

15. NUMBER OF PAGES
6

16. PRICE CODE

17. SECURITY CLASSIFICATION OF REPORT	18. SECURITY CLASSIFICATION OF THIS PAGE	19. SECURITY CLASSIFICATION OF ABSTRACT	20. LIMITATION OF ABSTRACT
UNCLASSIFIED	UNCLASSIFIED	UNCLASSIFIED	SAR